

# Static and dynamic mechanical properties of *Arundo Donax* fillers-epoxy composites



V. Fiore\*, T. Scalici, G. Vitale, A. Valenza

Department of "Ingegneria Civile, Ambientale, Aerospaziale, dei Materiali", University of Palermo, 90128 Palermo, Italy

## ARTICLE INFO

### Article history:

Received 26 September 2013

Accepted 9 January 2014

Available online 18 January 2014

### Keywords:

*Arundo Donax* fillers

Epoxy composites

Static properties

Dynamic mechanical analysis

Scanning electron microscope

Void content

## ABSTRACT

Aim of this work is to investigate the feasibility of using a natural and inexpensive filler obtained by grinding the culms of *Arundo Donax* as reinforcement of epoxy resins. The effect of the content and size of *Arundo Donax* fillers on static and dynamic mechanical properties was evaluated showing that the composites exhibit higher tensile moduli, comparable flexural moduli and lower strength properties in comparison to the neat resin. Moreover, changes in the storage and the loss moduli only above the glass transition temperature (i.e. in the rubbery region) were found while neither significant shifts of  $\tan \delta$  peaks to higher temperatures nor reductions in the peak height of the composites were also observed. To better understand the influence of *Arundo Donax* filler on the morphology of the composites, the analysis of the fractured surfaces using a scanning electron microscope and the assessment of void content were carried out. The results of this study shown that a new natural filler may be considered as possible reinforcement of epoxy composites useful in semi-structural applications.

© 2014 Elsevier Ltd. All rights reserved.

## 1. Introduction

The manufacturing of composite materials involve also the processing of raw material to obtain the basic constituents. Traditionally, the production of synthetic particles or fibres (e.g. glass, carbon or boron fibres) as reinforcement of thermosetting or thermoplastic polymers is strictly connected to expensive industrial processes, needed to get the required characteristics.

Moreover, the sustainability of a material is becoming an important feature in material technology regarding both the production phase (because of the immediate impact on man's health) and the end of the life cycle of a product (because of the environmental impact). For these reasons, over the last decade, polymers reinforced with natural fibres or particles have received ever increasing attention, both from the academic world and from several industries.

There is a wide range of different natural fibres which can be applied as reinforcements or fillers of polymer matrix: i.e. flax, hemp, jute, kenaf, coir, ramie and sisal, thanks to their properties and availability. Furthermore in these last year, some scientific works analyse the feasibility to use less common natural fibres [1], such like okra [2], betelnut [3], isora [4], artichoke [5], ferula [6] and buriti [7].

Although several studies on thermoplastic polymer filled with vegetable particles have been published [8–13], few research work regarding thermosetting resins can be found in the literature.

Raju and Kumarappa [14] studied the mechanical behavior of a novel bio-based composite materials prepared using groundnut shell particles as reinforcement of an epoxy resin, by varying the volume content and size of fillers. The authors showed that the highest tensile strength, tensile modulus, flexural strength and impact strength were observed for samples having 40% in volume and 0.5 mm size of groundnut shell particles. The highest flexural modulus was observed for samples reinforcement by 60% in volume of natural particles with size of 1 mm. Moreover they showed that water absorption decreases with increase in epoxy content.

Kumar [15] investigated the influence of the filler content on mechanical properties of epoxy resins reinforced by waste orange particles. It showed that maximum values of hardness, tensile, flexural and inter-laminar shear strengths are found for the composites prepared with weight content of filler equal to 20%.

Matejka et al. [16] focused on the evaluation of the friction–wear performances of non-asbestos organic composites containing jute fibres and powdered hazelnut shell. In this work it is found that the proper combination of natural materials (i.e. natural plant fibres and shells) can significantly improve the friction–wear performances of the composites.

The present paper explores the feasibility of using a natural and inexpensive material as *Arundo Donax* in order to obtain through simple processings (i.e. mechanical grinding and sieving) fillers for epoxy composites.

\* Corresponding author. Tel.: +39 091 23863721; fax: +39 091 7025020.

E-mail address: [vincenzo.fiore@unipa.it](mailto:vincenzo.fiore@unipa.it) (V. Fiore).

*Arundo Donax* is chosen since it is a non-wood plant that grows plenty and naturally in Sicily. Thanks to its high growth rate, it represents an invasive and aggressive species so its disposal is difficult.

To demonstrate the potential of this new natural filler, the static and dynamic mechanical behavior of *Arundo Donax* Fillers (ADFs)-epoxy composites were evaluated. Three compositions (5%, 10% and 15% in weight of ADFs) and four different ADFs sizes (<150  $\mu\text{m}$ , 150–300  $\mu\text{m}$ , 300–500  $\mu\text{m}$  and 500  $\mu\text{m}$ –2 mm) were investigated.

Static mechanical properties were obtained by carrying out tensile and three point bending tests. Dynamic characterization was carried out in tensile mode at 1 Hz frequency by heating the composites from room temperature to 160 °C.

To evaluate the void content of the manufactured composites, their real and theoretical densities were compared.

A scanning electron microscope (SEM) analysis was carried out to relate the macroscopic mechanical properties with the microstructural behavior of filler–matrix interface.

## 2. Material and methods

*Arundo Donax* culms were collected in a plantation in the area of Palermo (Sicily). After drying the fresh plant in open air, the reeds were cut into several pieces and then ground through a grinding machine. After that, *Arundo Donax* fillers (in the next ADFs) were sieved to obtain four fractions with different size (i.e. lower than 150  $\mu\text{m}$ , from 150  $\mu\text{m}$  to 300  $\mu\text{m}$ , from 300  $\mu\text{m}$  to 500  $\mu\text{m}$  and from 500  $\mu\text{m}$  to 2 mm). Finally, the ADFs were air-dried at 105 °C for 4 h and kept under dry atmosphere by using a desiccator just before the composites were manufactured. To reduce the cost and the technical issues associated with chemical treatments, the ADFs were not treated to improve filler–matrix interaction.

For each filler fraction investigated, composites with ADFs content equal to 5%, 10% and 15% in weight were manufactured.

An epoxy resin system obtained mixing a diglycid ether of bisphenol-A (DGEBA) epoxy monomer (SP 106, supplied by Gurit) with its own amine based curing agent (5:1 mix ratio by volume)

was used as matrix. As reported in the supplier datasheet, Table 1 shows the main properties of the components of the epoxy resin system. Control of neat epoxy resin was used as reference.

The ADFs were initially mixed with the resin into a flask and the mixture was placed under magnetic stirrer at 50 °C for one hour until a homogeneous blend was obtained. Then, the hardener was added to the mixture which was poured onto the cavities of silicon rubber mould so as to get samples for static and dynamic characterizations. The curing process was carried out at room temperature for 6 days. All the composites prepared in this study are presented in Table 2.

It is worth to note that it was not possible to manufacture composites with both high content (i.e. higher than 10%) and high filler size (i.e. higher than 300  $\mu\text{m}$ ), due to the high viscosity of the filler–resin blend. This limits its workability thus making not possible to pour the mix into the cavities of the mould. For the same reason, also the manufacturing of the composites with ADFs content higher than 10% and size higher than 300  $\mu\text{m}$ ) involves several difficulties. This probably influences both the morphological structure and consequently the mechanical behavior of these composites.

### 2.1. Assessment of void content

The real densities of the manufactured composites were measured using a helium pycnometer. For each composites, ten measures were carried out and average values of density were recorded. All deviation standards measured were lower to 0.01 g/cm<sup>3</sup>.

On the other hand, the theoretical densities of the composites were calculated [17].

The densities of natural fillers, measured using a helium pycnometer, were found to be 1.6532  $\pm$  0.0018 g/cm<sup>3</sup> for size range 0–150  $\mu\text{m}$ , 1.5480  $\pm$  0.0019 g/cm<sup>3</sup> for size range 150–300  $\mu\text{m}$ , 1.4655  $\pm$  0.0020 g/cm<sup>3</sup> for size range 300–500  $\mu\text{m}$ , 1.2296  $\pm$  0.0025 g/cm<sup>3</sup> for size range 500  $\mu\text{m}$ –2 mm.

The real density  $\rho_m$  of the reference samples (i.e. the neat resin), was equal to 1.1872  $\pm$  0.00005 g/cm<sup>3</sup>.

The volume void content ( $v_v$ ) of the manufactured composites was calculated by comparing their theoretical and real densities [17].

Voids are among the most common manufacturing-induced defects in composites. They are due mainly to the air entrapment during the composite manufacturing and to the moisture absorbed when the material is stored and processed. Higher void content usually means high susceptibility to water penetration in addition to both increased variation and poor strength properties of composites [18,19]. In particular, a good composite should have less

**Table 1**  
Main properties of the components of the epoxy resin system.

	Resin	Hardener
Viscosity at 25 °C (cP)	815	74
Density (g/cm <sup>3</sup> )	1.164	0.968
Boiling temperature (°C)	180	207
Ignition temperature (°C)	390	240
Vapour pressure at 20 °C (mbar)	0.5	0.5

**Table 2**  
Composites prepared in this study and their designations.

Designations	Filler size	Filler content (%)	Sample codes	Real density (g/cm <sup>3</sup> )	Theoretical density (g/cm <sup>3</sup> )	Voids content (%)
Neat resin	N.A.	0	Neat EP	1.1872	N.A.	N.A.
A	<150 $\mu\text{m}$	5	A-5	1.1887	1.2042	1.29
		10	A-10	1.1911	1.2217	2.50
		15	A-15	1.1889	1.2396	4.09
B	150–300 $\mu\text{m}$	5	B-5	1.1848	1.2012	1.36
		10	B-10	1.1824	1.2156	2.73
		15	B-15	1.1905	1.2302	3.23
C	300–500 $\mu\text{m}$	5	C-5	1.1798	1.1983	1.59
		10	C-10	1.1657	1.2097	3.64
		15	C-15	–	1.2212	–
D	500 $\mu\text{m}$ –2 mm	5	D-5	1.1601	1.1893	2.46
		10	D-10	1.1369	1.1913	4.57
		15	D-15	–	1.1934	–

than 1% voids, whereas a poorly made composite can have up to 5% void content [17].

## 2.2. Mechanical characterization

### 2.2.1. Tensile and flexural tests

Mechanical tests were performed according to ASTM: D638-10 (2010) and ASTM: D790-10 (2010) standards, using a Zwick-Roell Universal Testing Machine (UTM) equipped with a load cell of 5 kN. Five samples for each composite were tested in both the loading configurations. In particular, tensile tests were performed on dog-bone samples setting the crosshead speed equal to 5 mm/min.

Tensile strength and modulus were calculated according the ASTM: D638-10 (2010) standard.

Three point bending tests were carried out on prismatic samples (3.5 mm × 14 mm × 70 mm) setting the span length equal to 56 mm and the crosshead speed to 1.5 mm/min.

Flexural strength and modulus were calculated according the ASTM: D790-10 (2010) standard.

### 2.2.2. Dynamic mechanical analysis

Dynamic mechanical analysis was carried out using a Metravib dynamic mechanical analyzers model DMA<sup>+</sup>150, equipped with a load cell of 150 N.

The experiments were performed under the tensile mode at a frequency of 1 Hz. Prismatic samples of size 16 mm × 4 mm × 1 mm were used. The tests were conducted at temperatures from room to 200 °C with heating rate of 2 °C/min, under nitrogen atmosphere.

## 2.3. Microstructural analysis

Scanning electron microscopy (SEM) analysis was performed by scanning the fractures surfaces of dog-bone samples (i.e. those tested under tensile loading) using a SEM FEI Quanta 200 ESEM.

Before analysis, each sample was cut to a height of 10 mm, sputter-coated with a thin layer of gold and rubbed upon a 25-mm diameter aluminium disk.

## 3. Results and discussion

### 3.1. Assessment of void content

The theoretical and experimental densities of the composites with the corresponding void contents are shown in Table 2.

It is worth to note that the theoretical density values are not in agreement with the experimentally ones due to the presence of voids in the composites.

It is found that the void content increases with increasing filler content from 5% to 15%, regardless filler size. This may be due to fact that, with increasing filler content, the composites entrap more air during their manufacture by means of hand lay-up technique.

Moreover, for the composites with ADFs contents equal to 5% and 10%, void content increases with increasing filler size. Vice versa, the composites with 15% in weight of ADFs show decrements in void content with increasing filler size (i.e. from 4.9% to 3.23% for A-15 and B-15 composites, respectively). This weird behavior can be explained taking into account that the manufacturing of composites with filler content equal to 15%, as specified in Section 2, involved several difficulties due to the low workability of the blends.

It is possible to state that the composites with ADFs content equal to 5% in weight show a better morphology, i.e. void content lower than 2% (except D-5 composites having void content 2.46%).

On the other hand, the composites with ADFs content higher than 5% evidenced lower morphology quality than the previous ones, having void content higher than 2.5%.

## 3.2. Mechanical characterization

### 3.2.1. Tensile tests

In Figs. 1–3 the stress–strain curves, moduli and strengths of the composites and neat resin are respectively reported.

As reference, the neat resin show tensile modulus equal to  $2.17 \pm 0.11$  GPa and tensile strength to  $47.7 \pm 1.7$  MPa, respectively.

From Figs. 1 and 2, it is found that:

- The composites with ADFs size lower than 150 μm (i.e. A composites) show maximum tensile modulus, about 36% higher than the neat resin, for 10% in weight of ADFs.
- The tensile modulus increases with increasing filler content, for the composites reinforced with ADFs size within 150–300 μm range (B composites). In particular, the maximum value, about 40% higher than the neat resin, is reached for B-15 composites.

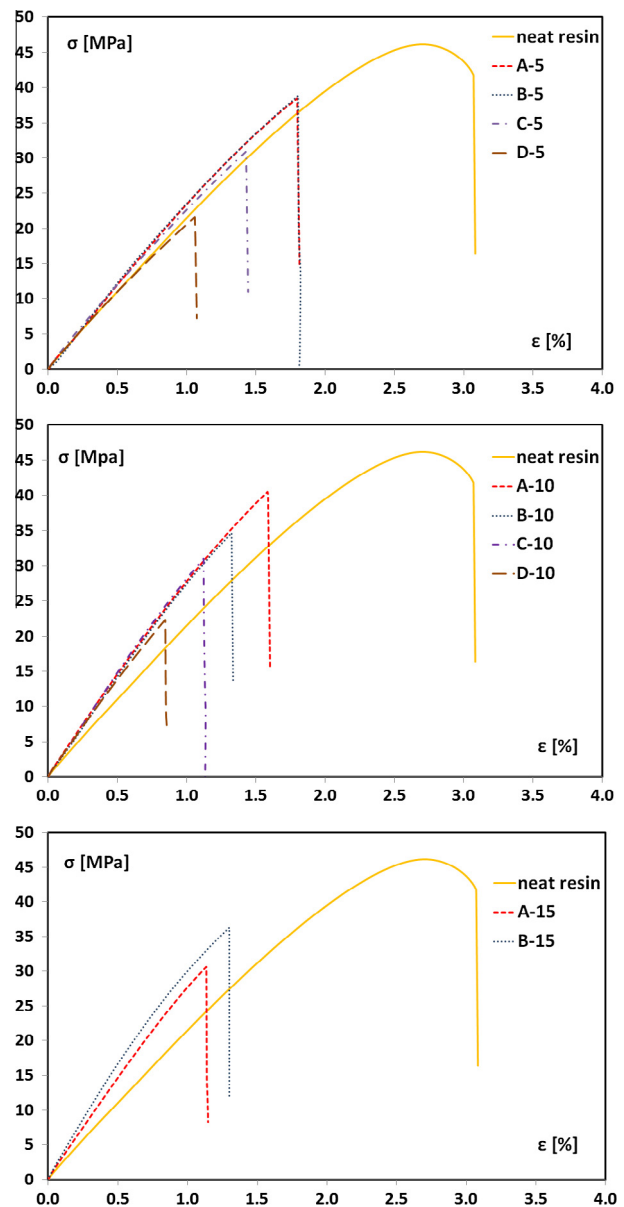


Fig. 1. Typical stress–strain curves obtained from tensile tests.

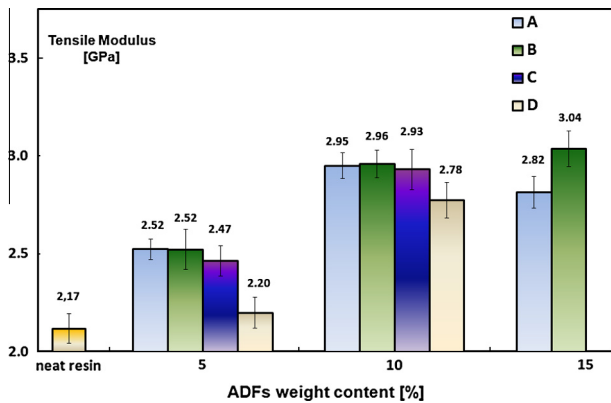


Fig. 2. Tensile modulus of the composites as function of ADFs weight content.

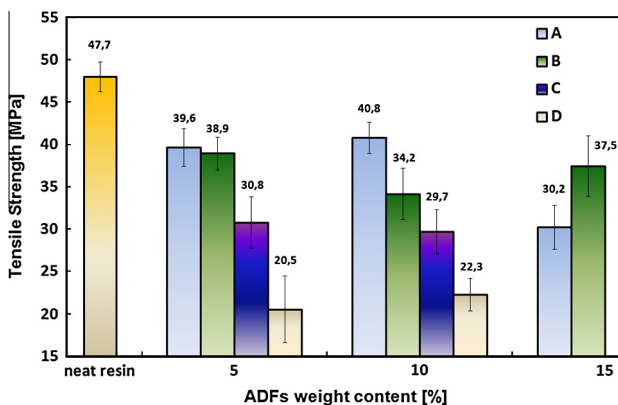


Fig. 3. Tensile strength of the composites as function of ADFs weight content.

- The composites reinforced with filler size higher than 300  $\mu\text{m}$  show increments of tensile modulus by varying the ADFs content from 5% to 10%.
- The tensile modulus does not vary with varying the ADFs size for the composites manufactured with 5% and 10% of filler content. Only the D-composites show lower tensile modulus.
- Regarding the composites with 15% filler content, the tensile modulus increases with increasing the ADFs size.
- The tensile modulus is observed to be highest for the B-15 composites, about 40% higher than the neat resin.

As general consideration, all the composites manufactured are found to show higher tensile moduli than the neat resin, except the D-5 composites. Consequently, it is possible to state that the *Arundo Donax* fillers can be useful as reinforcement to improve the tensile stiffness of the epoxy composites.

The improvements of the stiffness are due to the addition of a rigid filler in the epoxy resin.

As reported in literature [20,21], the modulus of composites depends only slightly on interfacial adhesion since it is measured at very small deformations.

As it will be better discussed in this section, the low compatibility between the hydrophilic natural filler and the hydrophobic epoxy resin leads to the reduction of the strength of the composites. However, small changes in the deformability of the matrix or that of the interphase do not influence the modulus much while the filler content dominates [22].

Lower tensile modulus shown by D-composites can be explained since large particles debond very easily under the effect of very small loads [23]. Thus, it is possible that debonding leads to the

formation of voids and the resulting material has a smaller stiffness.

Despite the positive effect on tensile modulus, the addition of ADFs involves instead detrimental effects on tensile strength of the composites (Figs. 1 and 3). All the composites investigated show lower tensile strengths than that of the neat resin. In particular, the maximum tensile strength, found for A-10 composites, is found to be 14.5% lower than that of the neat resin. Moreover, the presence of ADFs tends to decrease the elongation at break of the composites compared to the neat resin. This is probably due to the weak adhesion between vegetable fillers and thermosetting resins since no filler chemical treatments are carried out to improve the filler–matrix interaction. In fact it is well known [24–26] that the surface of natural fibres or fillers is hydrophilic (due mainly to the presence of amorphous cellulose and hemicelluloses) and therefore poorly suited for the use in hydrophobic polymer matrices like epoxy resins. This low compatibility results in weak interfaces that lead to internal strains, porosity, environmental degradation, moisture absorption and poor mechanical strengths of the composites [18],[19].

From Figs. 1 and 3, it is possible to evidence that:

- The composites with filler content equal to 5% and 10% in weight show decrements in tensile strength with increasing the size of ADFs.
- Minimum values of tensile strength are found for D-5 and D-10 composites, 57% and 53.3% lower than the neat resin, respectively.
- Vice versa, tensile strength of the composites with 15% of ADFs increases with increasing filler size.

These trends are related to void content within the manufactured composites. In particular (Table 2), it is worth to note that both the composites manufactured with ADFs content equal to 5% and 10% show increments of void content with increasing filler size, thus leading to the reduction of their tensile strength. Vice versa, tensile strength of the composites with 15% of filler content decreases with increasing the ADFs size, due to the decrement of void content.

### 3.2.2. Flexural tests

In Figs. 4–6 the stress–strain curves, moduli and strengths of the composites and neat resin are respectively reported. The neat resin shows flexural modulus equal to  $3.00 \pm 0.11$  GPa and flexural strength to  $87.5 \pm 3.7$  MPa, respectively.

The effect of content and size of ADFs on flexural modulus of the composites can be evidenced (Figs. 4 and 5):

- The composites with ADFs size lower than 150  $\mu\text{m}$  (i.e. the A composites) show maximum value of flexural modulus, 13.3% higher than the neat resin, for 10% content of ADFs.
- Flexural modulus increases with increasing filler content, for composites reinforced with ADFs size within 150–300  $\mu\text{m}$  range (i.e. the B composites).
- The composites with ADFs size higher than 300  $\mu\text{m}$  show increments of tensile modulus by varying the ADFs content from 5% to 10%.
- Flexural modulus remain almost constant with varying the ADFs size for the composites manufactured with 5% and 10% of filler content.
- Vice versa, the flexural modulus of the composites with 15% of filler content increases with increasing the ADFs size.
- Flexural modulus is observed to be highest for the C-10 composites, 15.3% higher than the neat resin.

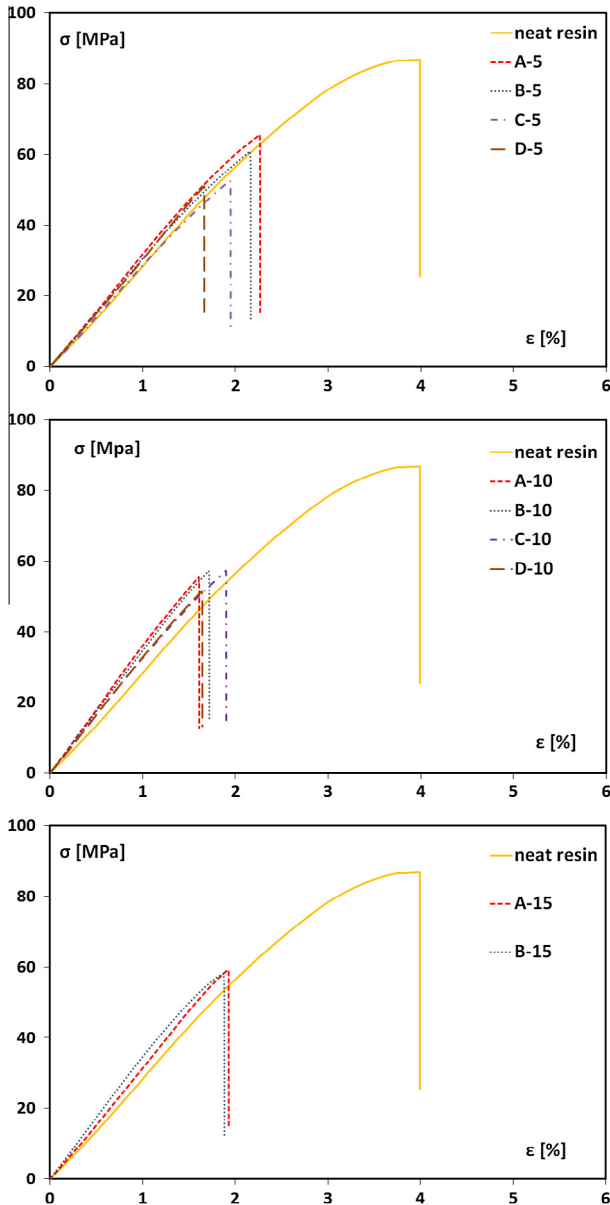


Fig. 4. Typical stress–strain curves obtained from flexural tests.

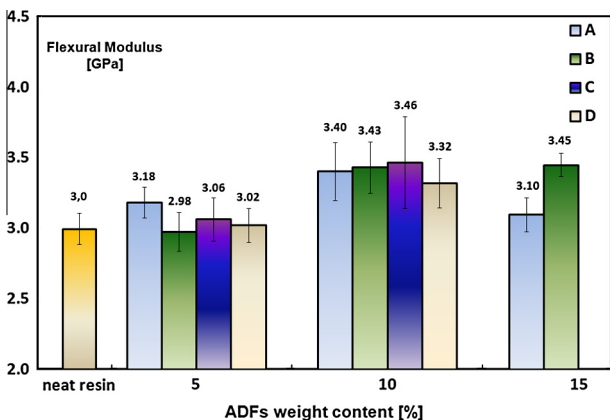


Fig. 5. Flexural modulus of the composites as function of ADFs weight content.

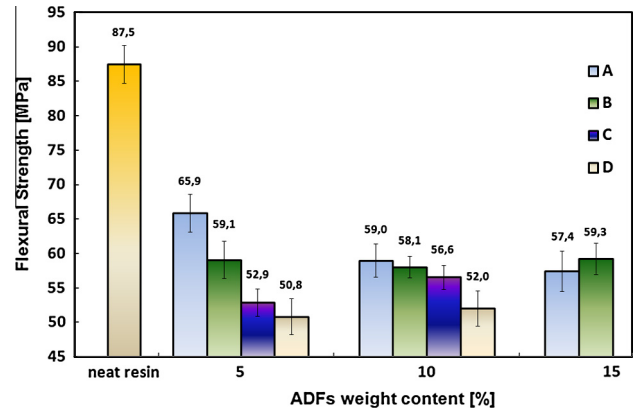


Fig. 6. Flexural strength of the composites as function of ADFs weight content.

As general consideration, the experimental data suggest that the changes in flexural moduli are substantially low in comparison with the modulus of the neat resin, which is indicative of the marginal effect of the presence of ADFs in modifying the flexural stiffness of the composites.

Also under flexural loading, the addition of the ADFs is found to involve detrimental effects on failure strength and deformation at break of the composites (Figs. 4 and 6). All the composites manufactured show lower flexural strengths in comparison with the neat resin. In particular, the maximum flexural strength, found for A-5 composites, is 24.7% lower than that of the neat resin.

As discussed in the previous section, the decrements in the strength properties is due to the poor adhesion between the hydrophilic filler and the hydrophobic epoxy resin that, vice versa, does not influence the stiffness of the composites. The presence of a rigid filler in the epoxy resin involves increments in the flexural stiffness.

Furthermore, it is worth to note that the flexural strength of the composites varies as function of the ADFs size similarly to the tensile strength (Fig. 3). In particular it is found that:

- The composites with filler content equal to 5% and 10% in weight show decrements in flexural strength with increasing size of ADFs.
- Minimum values of flexural strength are found for D-5 and D-10 composites, 42% and 40.6% lower than the neat resin, respectively.
- Vice versa, flexural strength of the composites with by 15% of ADFs increases with increasing filler size.

Similarly to the previous case, these trends are strictly connected with void content within the manufactured composites.

Based on EN standard 312-2 and 312-3 [27], the minimum requirements for flexural strength and modulus of panels for general purpose and interior fitments are 11.5 MPa and 1.6 GPa, respectively [14,28–29]. As shown in Figs. 5 and 6, all the composites satisfy these requirements.

### 3.2.3. Dynamic mechanical analysis

Fig. 7 shows the effect of ADFs size on the storage modulus  $E'$  of the composites filled with 5% in weight of *Arundo Donax*. The values of  $E'$  are found to be similar for all the investigated composites (~2.5 GPa) at low temperature (i.e. in the plastic region).

At higher temperatures, due to loss in stiffness of both the fillers and the matrix, the storage modulus drops. It is worth to note that  $E'$  increases with increasing filler size in the rubbery region. In

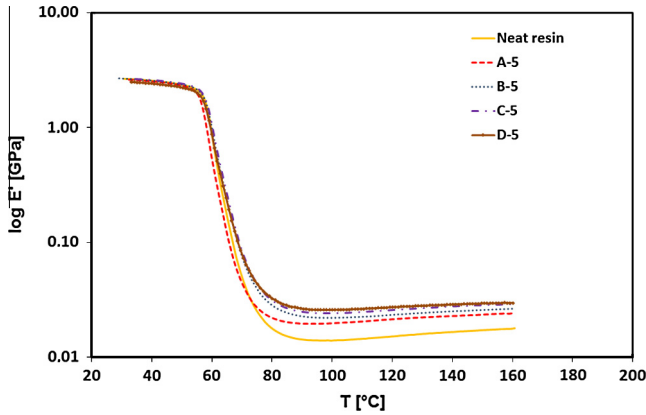


Fig. 7. Variation of storage modulus  $E'$  with temperature for the composites manufactured with 5% of ADFs.

particular,  $E'$  for the neat resin is 15.1 MPa at 120 °C whereas with incorporation of 5% of ADFs the storage modulus increases to 21.4 MPa (42% higher than the neat resin) for the A-5 composites, to 23.3 MPa (+54%) for the B-5 composites, to 25.7 MPa (+70%) for the C-5 composites and to 27.2 MPa (+80%) for the D-5 composites, respectively.

As shown in Fig. 8, similar considerations can be formulated for the composites with 10% and 15% of ADFs content.

As general consideration, the addition of *Arundo Donax* fillers do not influence  $E'$  of the composites in the plastic region, regardless of both the size and content. On the other hand,  $E'$  increases with increasing both size and content of ADFs in the rubbery region.

In particular the storage modulus at 120 °C of the composites with filler size lower than 150  $\mu\text{m}$ , increases to 21.4 MPa (+42% higher than the neat resin) for the A-5 composites, to 29.7 MPa (+96% higher than the neat resin) for the A-10 composites and to 31.8 MPa (+110%) for the A-15 composites, respectively.

Regarding the composites reinforced with filler size within the range between 150  $\mu\text{m}$  and 300  $\mu\text{m}$ ,  $E'$  at 120 °C increases to 23.3 MPa (+54% higher than the neat resin) for the B-5 composites, to 36.1 MPa (+139% higher than the neat resin) for the B-10 composites and to 47.2 MPa (+212%) for the B-15 composites, respectively.

Similar trends are also observed for the composites filled with particles of size higher than 300  $\mu\text{m}$ .

Loss modulus  $E''$  represents the viscous response of the material. Fig. 9 shows the variations of  $E''$  of the composites manufactured with 10% of ADFs, as function of temperature. Similar trends are observed for the composites filled with 5% and 15% in weight of ADFs, respectively.

It can be noted that loss modulus increased in the plastic region and then decreased with increasing temperature in the rubbery region.

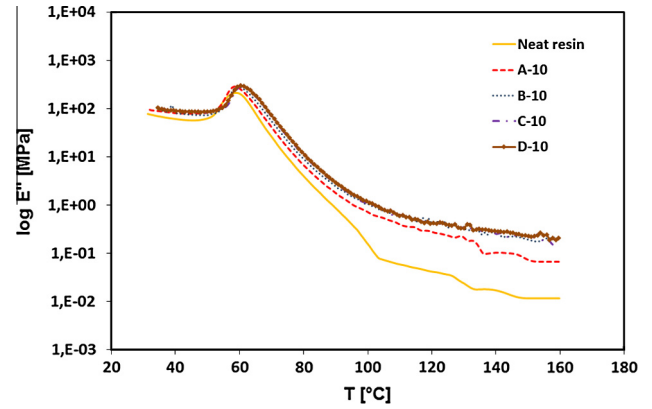


Fig. 9. Variation of loss modulus  $E''$  with temperature for the composites manufactured with 10% of ADFs.

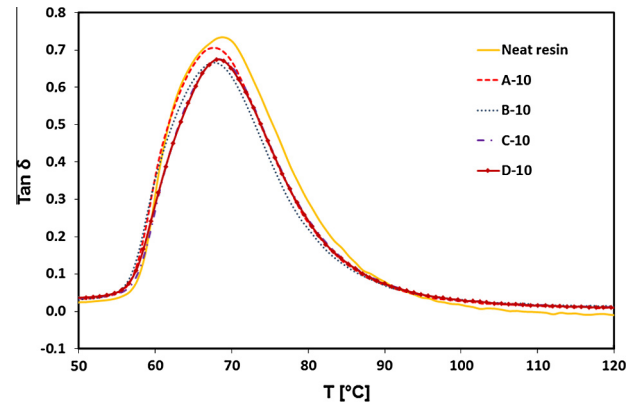


Fig. 10. Variation of  $\tan \delta$  with temperature for the composites manufactured with 10% of ADFs.

The effect of the ADFs size is found to influence more on the value of  $E''$  above the glass transition temperatures (i.e. temperature at peak values of  $E''$ ). In particular, in the plastic region all the composites show values of  $E''$  equal about to 100 MPa, slightly higher than the neat resin, regardless of the ADFs size. In the rubbery region  $E''$  increases with increasing the ADFs size.

Similarly, the loss modulus is not influenced by ADFs content in the plastic region whereas it increases with increase of filler content above the glass transition temperature.

$\tan \delta$ , also named damping, can be determined by the ratio between the loss modulus and the storage modulus ( $E''/E'$ ). It depends on the filler–matrix adhesion: i.e. a weak filler–matrix adhesion leads to higher values of  $\tan \delta$  [30,31] while a good

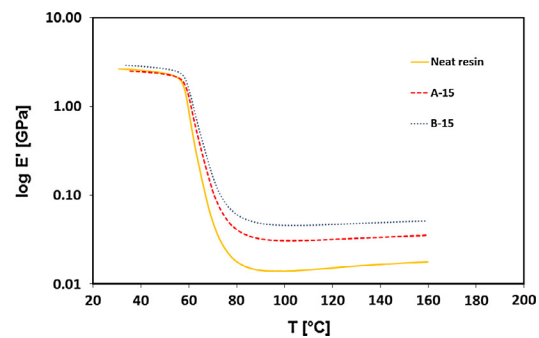
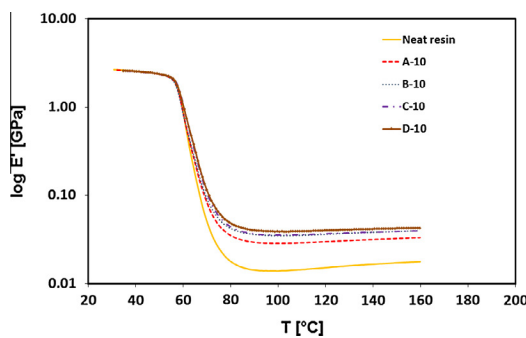
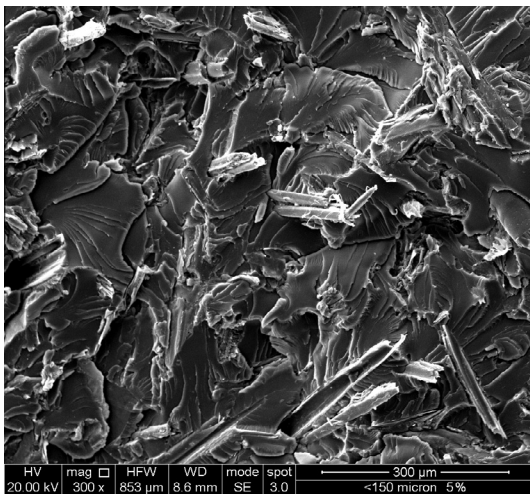


Fig. 8. Variation of storage modulus  $E'$  with temperature for the composites manufactured with (a) 10% and (b) 15% of ADFs.

**Table 3**  
Peak height of damping and  $T_g$  obtained from  $\tan \delta$  curves and  $E''$  curves.

Composites	Peak height of damping	$T_g$ from $\tan \delta$ curve (°C)	$T_g$ from $E''$ curve (°C)
Neat resin	0.734	69.1	60.50
A-5	0.732	66.3	58.7
A-10	0.706	67.4	58.8
A-15	0.706	68.85	61.2
B-5	0.733	68.4	60.7
B-10	0.667	67.55	59.9
B-15	0.687	69.1	61.45
C-5	0.728	68.95	60.4
C-10	0.675	68.45	60.8
C-15	–	–	–
D-5	0.678	67.6	60.0
D-10	0.675	68	60.4
D-15	–	–	–



**Fig. 11.** Fracture surface micrograph of A-5 composites.

filler–matrix adhesion limits the mobility of the polymer chains thus reducing the damping.

Fig. 10 shows that ADFs slightly reduces  $\tan \delta$ , thus confirming the presence of weak adhesion between the hydrophilic filler and the hydrophobic polymer used as matrix. Similar trends of  $\tan \delta$  are also observed for the composites filled with 5% and 15% in weight of ADFs, respectively.

The glass transition temperature  $T_g$  can be calculated as the temperature at which the damping [30,32] or the loss modulus

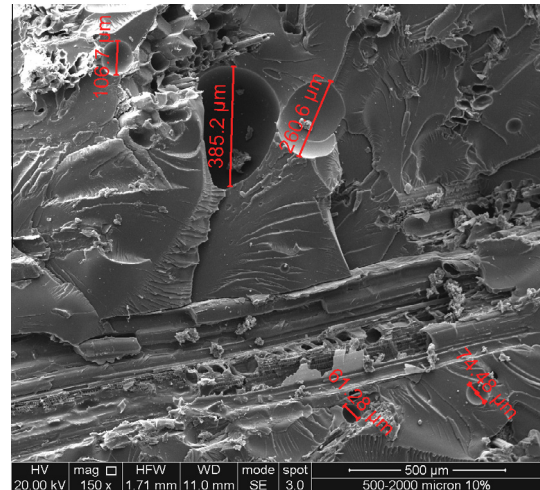


**Fig. 13.** Fracture surface micrograph of D-10 composites.

[33–35] attain their maximum values. As shown in Table 3, the glass transition temperature is not influenced neither by the ADFs size nor by their content. In particular, the  $T_g$  varies from 69.1 °C for the neat resin to the range between 66.3 °C and 69.1 °C for the composites, thus no shift of  $T_g$  to higher temperatures can be attributed to the presence of the ADFs.

This means that the presence of the ADFs does not reduce the mobility of the matrix chains, due to the weak filler–matrix interfacial adhesion.

### 3.3. Microstructural analysis

Scanning electron microscopy (SEM) analysis was performed by scanning the tensile fractured surfaces of the composites to better understand the influence of the ADFs on their morphology.

SEM analysis is an excellent technique for examining the surface morphology of samples. It allows to deeper analyse the filler–matrix interfacial adhesion, to focus how many voids are dispersed and to evaluate their size at varying the filler size and content.

As shown in Fig. 11, the fractured surface of the A-5 composites is not characterized by voids or pores. This image highlights their good morphology, already evidenced by the assessment of void content (i.e. 1.29%). The B-5 composites (void content  $v_v$  equal to 1.36%) and the C-5 composites ( $v_v = 1.59\%$ ) show similar morphologies to the previous one, so the related micrographs are not shown.

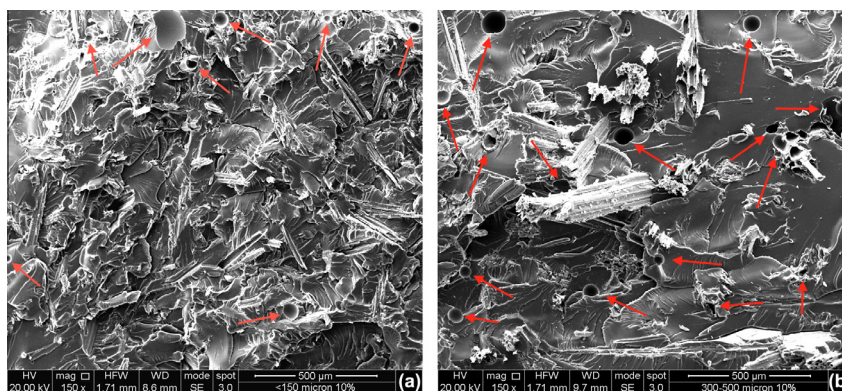


**Fig. 12.** Fracture surface micrographs of (a) A-10 and (b) C-10 composites.

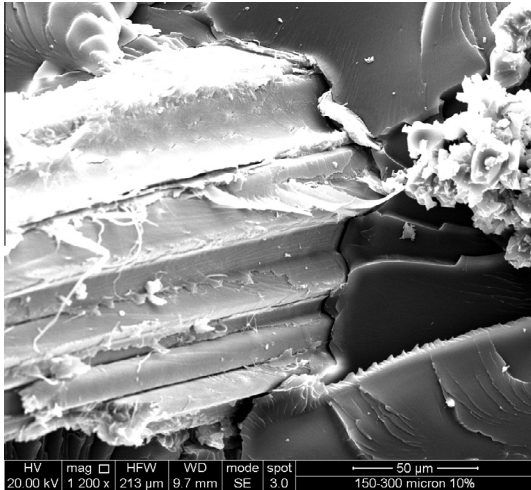


Fig. 14. High magnification micrograph of filler–matrix interface.

A certain number of micro-voids can be highlighted on the fractured surfaces of the composites reinforced with filler content equal to 10% in weight and filler size lower than 150 µm (Fig. 12a) and within the range 300–500 µm (Fig. 12b).

The micrographs allow to evidence the different morphologies of the A-10 composites and the C-10 composites. In particular, the A-10 composites ( $v_v = 2.5\%$ ) appear to be characterized by a lower number of micro-voids than the C-10 composites ( $v_v = 3.64\%$ ). No notable differences in the dimension of voids can be observed. The morphologies of the B-10 composites ( $v_v = 2.73\%$ ) and D-5 composites ( $v_v = 2.46\%$ ), appear similar to that of the A-10 composites, so are not shown for sake of conciseness.

On the other hand, the fractured surface of the D-10 composites (Fig. 13) shows both micro-voids (<100 µm) and voids of higher dimensions (i.e. >200 µm). The high void content (i.e. 4.57%) measured for the D-10 composites is due to the presence of these macro-voids.

In Fig. 14 the micrograph at high magnification of an embedded fibre is shown. The morphology clearly evidences the weak filler–matrix adhesion, due to the low compatibility between the hydrophilic filler and the hydrophobic polymer used as matrix. As discussed in the Section 3.2, this low compatibility leads to poor strength properties of the ADFs–epoxy composites studied.

#### 4. Conclusions

The crucial scope of this work was to manufacture epoxy composites using a natural and inexpensive filler derived from the culms of *Arundo Donax*.

In particular, the influence of the content and size of ADFs on static and dynamic mechanical properties of the composites was investigated.

Three compositions (5%, 10% and 15% fillers weight content) and four different filler sizes (<150 µm, 150–300 µm, 300–500 µm and 500 µm–2 mm) were analyzed.

The static mechanical characterization shows that:

- All the composites show higher tensile moduli than the neat resin.
- Tensile modulus is observed to be highest for B-15 composites (40% higher than the neat resin).
- All the composites show comparable or slightly higher flexural moduli than the neat resin.
- Flexural modulus is observed to be highest for C-10 composites (15.3% higher than the neat resin).

- All the composites show lower tensile and flexural strengths than the neat resin.
- The mechanical strengths of the composites with ADFs content equal to 5% and 10% decreases with increasing filler size.
- Vice versa, the mechanical strengths of the composites with ADFs content equal to 15% and 10% increases with increasing filler size.

Thus, the ADFs can be useful to improve the tensile stiffness of the composites whereas they have a marginal effect in modifying the flexural stiffness of the composites.

The detrimental effects on strength properties of the composites are due to the poor adhesion between the hydrophilic filler and the hydrophobic matrix since no filler chemical treatments are carried out to improve the filler–matrix interaction.

Furthermore, it is worth to note that the variations of the strength properties as function of size and content of ADFs are strictly related to void content within the composites.

The composites were also tested for its dynamic mechanical properties and following are the conclusions:

- Neither changes in storage modulus nor in loss modulus can be attributed to the presence of the ADFs in the plastic region.
- Both storage modulus and loss modulus increase with increasing both size and content of the ADFs in the rubbery region.
- Neither significant shifts of  $\tan \delta$  peaks to higher temperatures nor reductions in the peak height of damping are found.

These results confirm that the addition of the ADFs does not reduce the mobility of the matrix chains, due to the weak filler–matrix interfacial adhesion.

S.E.M. analysis allowed to analyse filler–matrix interface highlighting the weak compatibility between the natural filler and the epoxy resin used as matrix. Furthermore, different morphologies of the composites manufactured at varying size and content of fillers were evidenced.

It can be conclude that the new filler made out by grinding the culms of *Arundo Donax* may be considered as a possible alternative of synthetic fillers or other natural fillers to manufacture epoxy composites useful in semi-structural applications. Furthermore, the use of *Arundo Donax* as raw material will improve the opportunity of disposal of this invasive and aggressive non-wood plant.

#### References

- [1] Monteiro SN, Calado V, Margem FM, Rodriguez RJS. Thermogravimetric stability behavior of less common lignocellulosic fibers – a review. *J Mater Res Technol* 2012;01:189–99.
- [2] De Rosa IM, Kenny JM, Puglia D, Santulli C, Sarasini F. Morphological, thermal and mechanical characterization of okra (*Abelmoschus esculentus*) fibres as potential reinforcement in polymer composites. *Compos Sci Technol* 2010;70:1116–22.
- [3] Yousif BF, Nirmal U, Wong KJ. Three-body abrasion on wear and frictional performance of treated betelnut fibre reinforced epoxy (T-BFRE) composite. *Mater Des* 2010;31:4514–21.
- [4] Mathew L, Joseph KU, Joseph R. Isora fibre: morphology, chemical composition, surface modification, physical, mechanical and thermal properties – a potential natural reinforcement. *J Nat Fibres* 2006;3:13–27.
- [5] Fiore V, Valenza A, Di Bella G. Artichoke (*Cynara cardunculus* L.) fibres as potential reinforcement of composite structures. *Compos Sci Technol* 2011;71:1138–44.
- [6] Seki Y, Sarikanat M, Sever K, Durmuşkahya C. Extraction and properties of *Ferula communis* (chakshir) fibers as novel reinforcement for composites materials. *Composites Part B* 2013;44:517–23.
- [7] Monteiro SN, Lopes FPD, Costa LL, Motta LC, Lopes LF, Vasconcellos LS. Study of the buriti waste fiber as a possible reinforcement of polyester composites. In: Proceedings of REWAS 2008: global symposium on recycling, waste treatment and clean technology. p. 517–22.
- [8] Bledzki AK, Reihmane S, Gassan J. Thermoplastics reinforced with wood fillers: a literature review. *Polym Plast Technol Eng* 1998;37:451–68.
- [9] Espert A, Vilaplana F, Karlsson S. Comparison of water absorption in natural cellulosic fibres from wood and one-year crops in polypropylene composites

- and its influence on their mechanical properties. *Composites Part A* 2004;35:1267–76.
- [10] La Mantia FP, Morreale M. Green composites: a brief review. *Composites Part A* 2011;42:579–88.
- [11] Khalid M, Ratnam CT, Chuah TG, Ali S, Choong TSY. Comparative study of polypropylene composites reinforced with oil palm empty fruit bunch fiber and oil palm derived cellulose. *Mater Des* 2008;29:173–8.
- [12] Essabir H, Hilali E, Elgharad A, El Minor H, Imad A, Elamraoui A, et al. Mechanical and thermal properties of bio-composites based on polypropylene reinforced with nut-shells of argan particles. *Mater Des* 2013;49:442–8.
- [13] Essabir H, Nekhlaoui S, Malha M, Bensalah MO, Arrakhiz FZ, Qaiss A, et al. Bio-composites based on polypropylene reinforced with almond shells particles: mechanical and thermal properties. *Mater Des* 2013;51:225–30.
- [14] Raju GU, Kumarappa S. Experimental study on mechanical properties of groundnut shell particle-reinforced epoxy composites. *J Reinf Plast Compos* 2011;30:1029–37.
- [15] Kumar P. Mechanical behavior of orange peel reinforced epoxy composite. B.Tech Thesis, In Department of Mechanical Engineering, National Institute of Technology Rourkela, 2012.
- [16] Matějka V, Fu Z, Kukutschová J, Qi S, Jiang S, Zhang X, et al. Jute fibers and powdered hazelnut shells as natural fillers in non-asbestos organic non-metallic friction composites. *Mater Des* 2013;51:847–53.
- [17] Agarwal BD, Broutman LJ. Analysis and performance of fiber composites. 2nd ed. New York: John Wiley & Sons; 1990.
- [18] Abdullah NM, Ahmad I. Potential of using polyester reinforced coconut fiber composites derived from recycling polyethylene terephthalate (PET) waste. *Fibers Polym* 2013;14:584–90.
- [19] Vilay V, Mariatti M, Mat Taib R, Todo M. Effect of fiber surface treatment and fiber loading on the properties of bagasse fiber-reinforced unsaturated polyester composites. *Compos Sci Technol* 2008;68:631–8.
- [20] Dányádi L, Renner K, Szabó Z, Nagy G, Móczó J, Pukánszky B. Wood flour filled PP composites: adhesion, deformation, failure. *Polym Adv Technol* 2006;17:967–74.
- [21] Renner K, Móczó J, Pukánszky B. Deformation and failure of PP composites reinforced with lignocellulosic fibers: effect of inherent strength of the particles. *Compos Sci Technol* 2009;69:1653–9.
- [22] Faludi G, Dora G, Renner K, Móczó J, Pukánszky B. Improving interfacial adhesion in pla/wood biocomposites. *Compos Sci Technol* 2013;89:77–82.
- [23] Dányádi L, Renner K, Móczó J, Pukánszky B. Wood flour filled polypropylene composites: interfacial adhesion and micromechanical deformations. *Polym Eng Sci* 2007;47:1246–55.
- [24] Doan TTL, Brodowsky H, Mäder E. Jute fibre/epoxy composites: surface properties and interfacial adhesion. *Compos Sci Technol* 2012;72:1160–6.
- [25] Alsaed T, Yousif BF, Ku H. The potential of using date palm fibres as reinforcement for polymeric composites. *Mater Des* 2013;43:177–84.
- [26] Suradi SS, Yunus RM, Beg MDH. Oil palm bio-fiber-reinforced polypropylene composites: Effects of alkali fiber treatment and coupling agents. *J Comp Mater* 2011;45:1853–61.
- [27] EN 312:2003. Particleboards-specifications. European Committee for Standardization.
- [28] Lu JZ, Wu QL, Negulescu II, Chen Y. The influences of fiber feature and polymer melt index on mechanical properties of sugarcane fiber/polymer composites. *J Appl Polym Sci* 2006;102:5607–19.
- [29] Akgül M, Güler C, Üner B. Opportunities in utilization of agricultural residues in bio-composite production: corn stalk and oak wood fiber in medium density fiberboard. *Afr J Biotechnol* 2010;9:5090–8.
- [30] Shanmugam D, Thiruchitrabalam M. Static and dynamic mechanical properties of alkali treated unidirectional continuous palmyra palm leaf stalk fiber/jute fiber reinforced hybrid polyester composites. *Mater Des* 2013;50:533–42.
- [31] Martinez-Hernandez AL, Velasco-Santos, De Icaza M, Victor MC. Dynamic mechanical and thermal analysis of polymeric composites reinforced with keratin biofibers from chicken feathers. *Composites: Part B* 2007;38:405–10.
- [32] Manikandan-Nair KC, Thomas S, Groeninckx G. Thermal and dynamic mechanical analysis of polystyrene composites reinforced with short sisal fibres. *Compos Sci Technol* 2001;61:2519–29.
- [33] Saha AK, Das S, Bata D, Mitra BC. Study of jute fiber reinforced polyester composites by dynamic mechanical analysis. *J Appl Polym Sci* 1999;71:1505–13.
- [34] Ray D, Sarkar BK, Das S, Rana AK. Dynamic mechanical and thermal analysis of vinyl ester-resin-matrix composites reinforced with untreated jute fibres. *Compos Sci Technol* 2002;62:911–7.
- [35] Sudhir KS, Gautam S, Aru C. Dynamic mechanical analysis of randomly oriented short bagasse/coir hybrid fiber reinforced epoxy novolac composites. *Fiber Polym* 2011;12:506–13.